IN-34

136216

P.14

Second-Order Closure Modeling of Turbulent Buoyant Wall Plumes

Gang Zhu and Ming-Chia Lai
Wayne State University
Detroit, Michigan

and

Tsan-Hsing Shih
NASA Lewis Research Center
Cleveland, Ohio

December 1992

NASA

ICOMP
INSTITUTE FOR COMPUTATIONAL MECHANICS IN PROPULSION
NASA
Lewis Research Center
Case Western
Reserve University
Ohio Aerospace
Institute

Second-Order Closure Modeling of Turbulent Buoyant Wall Plumes

Gang Zhu, Ming-Chia Lai*
Mechanical Engineering Department
Wayne State University
Detroit, Michigan

Tsan-Shin Shih
Center for Modeling of
Turbulance and Transition
NASA/Lewis Research Center
Cleveland, Ohio

ABSTRACT

Non-intrusive measurements of scalar and momentum transport in turbulent wall plumes, using a combined technique of laser Doppler anemometry and laser-induced fluorescence, has shown some interesting features not present in the free jets or plumes. First, buoyancy-generation of turbulence is shown to be important throughout the flow field. Combined with low-Reynolds-number turbulence and near-wall effect, this may raise the anisotropic turbulence structure beyond the prediction of eddy-viscosity models. Second, the transverse scalar fluxes do not correspond only to the mean scalar gradients, as would be expected from gradient-diffusion modeling. Third, higher-order velocity-scalar correlations which describe turbulent transport phenomena could not be predicted using simple turbulence models.

A second-order closure simulation of turbulent adiabatic wall plumes, taking into account of the recent progress in scalar transport, near-wall effect and buoyancy, is reported in the current study to compare with the non-intrusive measurements. In spite of the small velocity scale of the wall plumes, the results showed that low-Reynolds-number correction is not critically important to predict the adiabatic cases tested and cannot be applied beyond the maximum velocity location. The mean and turbulent velocity profiles are very closely predicted by the second-order closure models. But the scalar field is less satisfactory, with the scalar fluctuation level underpredicted. Strong intermittency of the low-Reynolds-number flow field is suspected of these discrepancies. The trends in second- and third-order velocity-scalar correlations, which describe turbulent transport phenomena, are also predicted in general, with the cross-streamwise correlations better than the streamwise one. Buoyancy terms modeling the pressure-correlation are shown to improve the prediction slightly. The effects of equilibrium time-scale ratio and boundary condition are also discussed.

---

* Assist. Professor, ASME member

INTRODUCTION

Wall plumes are encountered above fires along surfaces, near baseboard heaters and electronic circuit boards, and in other confined natural convection processes. Turbulent wall plumes, although simple in geometry, are also a fundamentally interesting yet complicated flow. Wall jet has the characteristics of both boundary layers and free jets. Wall plumes are further complicated by buoyancy. It is characterized by intermittent, low-Reynolds-number and large-scale turbulence, involving the interactions of buoyancy, turbulence, and the damping effect of a solid surface. Therefore, predicting this flow poses a great challenge. In addition, wall plumes provide an excellent opportunity for studying these interactions, since they are relatively thick, reducing problems of spatial resolution, but do not exhibit the effects of large-scale disturbances (flapping) encountered in free plumes, due to the stabilizing effect of the wall.

Past measurements of wall plume turbulence properties are very limited. Grella and Faeth (1975) used hot-wire anemometry to measure streamwise velocity fluctuations in turbulent adiabatic wall plumes. Liburdy and Faeth (1978) and Liburdy et al. (1979) studied turbulent thermal plumes along a vertical isothermal wall. Hot-wire anemometry was also used to measure mean and fluctuating velocities and temperatures and their correlations. However, these studies have several limitations, and no data are available to confirm them. First of all, parasitic heat losses from thermal wall plumes are difficult to control; therefore, adiabatic conditions were only approximated by Grella and Faeth (1975). Furthermore, intrusive probes are not very reliable for measuring the properties of wall plumes. Probes have large uncertainties when turbulence intensities are high, and near surfaces; therefore, properties are only measured reliably in a narrow region of the flow. Probes also disturb the flow, particularly near the edge, where flow reversals occur (Lai et al., 1986).

Lai et al. (1986, 1987) reported the first non-intrusive measurements of mean and fluctuating velocities and scalars, as well as their correlations in turbulent adiabatic wall plumes. Problems associated with past experiments were eliminated entirely. Since

the data of this experimental program is used to validate the SOC model in the present study, a brief summary is provided in the following section. These flows were analyzed using both mixing-length model and simplified k-ϵ-f model with wall function but ignoring buoyancy/turbulence interactions entirely, similar to past analyses of buoyant round diffusion flames (Jeng et al., 1982; Jeng and Faeth, 1984). Both methods yielded satisfactory predictions of mean quantities in spite of the effects of low-Re and large-scale coherent structures seen in the flow visualizations. However, turbulent fluctuations were underestimated. This was attributed to the effects of buoyancy/turbulence interactions by analysis of the production budget in the k-equation using velocity/scalar correlations. Due to the small velocity scale of wall plumes, the y^+ at the maximum velocity point y_m is well inside the buffer layer (ca. 18); even at the outer edge of the flow y^+ is very small (ca. 150, using u_τ as defined by Kruka and Eskinazi (1964) for wall jet). This puts the first grid literally within the laminar sublayer. Therefore, in spite of the apparent success, implementation of the wall function in k-ϵ-f model for wall plumes is debatable.

However, interesting features of the flow properties remain beyond the prediction of the eddy-viscosity models, such as mixing-length or k-ϵ-f models. For example, the anisotropic turbulence intensities in the streamwise (open symbols) and transverse (closed symbols) direction cannot be predicted. Even no counter-gradient diffusion is observed in the measurements, the transverse scalar fluxes do not correspond to the mean scalar gradients, as would be expected from the gradient-diffusion assumption in eddy-viscosity models (Lai, 1985). Therefore, the diffusion models based on the first principle as suggested by Lumley for SOC model is preferred over the simple gradient-diffusion assumption for the eddy-viscosity models.

In addition, higher-order velocity-scalar correlations which describe turbulent transport phenomena could not be predicted using simple turbulence models. Triple moments dominate the diffusion terms in the second moment equations; for example, $<u_i u_j u_k>$, $<f u_i u_j>$ and $<f^2 u_k>$ appear in the second-moment equations for the Reynolds stress $<u_i u_j>$, scalar flux $<f u_i>$ and scalar variance $<f^2>$. These correlation measurements would therefore validate and provide new insight into modeling of the scalar transport processes.

One possibility is to apply the algebraic stress model, which is considered a modified version of the k-ϵ model without the gradient-diffusion assumption (Rodi, 1972, and Gibson and Launder, 1978). Therefore, the algebraic model could have a wider range of applicability than the eddy-viscosity models, although the assumption used in deriving this model needs further justification. There are already some buoyant flows considered with the algebraic model. For example: buoyancy-modified free surface flows (Gibson and Launder, 1976, Hossain and Rodi, 1977, and McGuirk and Papadimitriou, 1985); natural convection on a flat plate and a heated cavity (Humphrey and To, 1985, 1986, and To and Humphrey, 1986); and a developing buoyant plume (McGuirk and Papadimitriou, 1985). However, no complete second-order closure (SOC) simulation has been performed, on the two-dimensional wall plumes.

The recent renewed effort in SOC models, aiming at improving the physical ingredients of second-moment closure schemes, as reviewed by Launder (1989), holds promise for improving the reliability with which we can predict industrially interesting flows. Unlike previous models, second-order closure models directly solve the transport equations for Reynolds stresses and scalar fluxes. In order to close the system equation, a number of terms must be modeled, such as the third order moments, the pressure-correlations, and the transport terms for dissipation rates. Various models have been proposed for these terms (Daly and Harlow 1970, Hanjalic

and Launder, 1972, and Lumley, 1978). The first-principle-based diffusion terms by Lumley has been shown to produce more realistic behaviors in wall plumes (Lai and Jeng, 1990). Current development is primarily attributed to Lumley's extensive article (1978), which is based on tensorial algebra, realizability concept and first principle modeling of diffusion terms. Further impetus is given by the direct numerical simulation efforts that have been emerging over the past five years from the Stanford/NASA Ames Research conglomerate. Noteworthy developments are in progress contributing to the area of scalar transport, such as: pressure-correlation, diffusive transport, dissipation and near-wall effect.

The whole area of low-Re near-wall turbulence is one where the scalar flux development lags well behind that of the Reynolds stresses, even for flow parallel to a wall. A consistent low-Re treatment of both the velocities and scalar is currently in progress (Shih and Mansour, 1990, 1992, Shima, 1988, and Launder and Shima, 1990), aided by direct numerical simulation data (Kim and Moin, 1987, and Rogers et al., 1986). The goal of the present study is, therefore, to validate the performance of SOC models on a turbulent adiabatic wall plume, based on Lai's (1985) data. The model considered incorporates recent developments in modeling scalar transport, pressure-correlation, low-Re and buoyant flows.

THE EXPERIMENTAL PROGRAM

This section briefly summarized the experimental program, with emphasis on the combined velocity-scalar measurements. A full account of the complete experimental program is provided by Lai (1985). The test flow was generated by well-mixed carbon dioxide/air flowing downward along a plane wall in still air. The carbon dioxide/air mixture entered a plenum at the top of the wall and then passed through a series of baffles to achieve a uniform two-dimensional flow at the 21-mm-high exit slot. The test wall was 1000mm long and 800mm wide, and had 305-mm-high side walls to help preserve two-dimensionality. Windows in the side walls provided optical access for structure measurements at $x/b = 0.1$ (the initial condition), 10, 20, and 37.5.

Gas flow to the top of the wall was provided by an oil-free air compressor and commercial-grade carbon dioxide stored in cylinders. Flows were controlled by pressure regulators and metered by critical-flow orifices. After mixing, the flow passed through a 25mm($id.$) × 37m long tube to ensure complete mixing and equilibration to local room temperatures. Uncertainties in flow measurements and initial gas composition were less than three percent. In the experiments reported here the density ratios of the carbon dioxide/air mixture (at the exit slot) to the ambient air were 1.02 and 1.04. The mean velocities at the exit slot were set at 0.31 and 0.43m/s respectively, to match an asymptotic Froude number of 5, which is similar to the one measured by Grella and Faeth (1975) for vertical adiabatic wall plumes. This is confirmed by the fact that the maximum mean velocities measured at the furthest downstream position are almost the same as those at the slot exit. Therefore, the flow neither under-nor over-accelerated at the slot exit, which reduces the distance for flow development.

A combined laser Doppler anemometry and laser-induced fluorescence (LDA/LIF) system was used to measure the velocity and scalar (mixture fraction) simultaneously; see Lai and Faeth (1987) for a detailed description of the arrangement. Iodine vapor was seeded in the flow to provide the LIF signal, while aluminum oxide particles (around 500 nm diameter) were seeded in both the slot and the ambient gases for the LDA system. The LIF signal was separated from light scattered from the laser line using long-pass optical filters. The LDA and LIF were both sampled for 100 sec-

onds at $80Hz$ using a low-pass anti-aliasing filter with a 40 Hz cutoff frequency. Measurements of power spectral densities of scalar fluctuations showed that power spectra were on the order of 0.1 percent of maximum value at $40Hz$ at the worst (Lai, 1985); therefore, the frequency response of this system was adequate. The signals were processed to yield time averages; however, the distinction between Favre and time-averaged quantities is small for these flows (less than five percent).

The measurements are estimated to have the following experimental uncertainties (95 percent confidence): mean and fluctuating velocities less than four and six percent, mean and fluctuating concentrations less than five and ten percent, Reynolds stress less than twenty percent, and turbulent mass fluxes (second-order correlation of velocity and scalar) less than fifteen percent. These estimates are based on the maximum value of each quantity and are proportionately higher elsewhere. Higher-order correlations have even larger uncertainties, which can be estimated from these estimates using conventional error-propagation analysis.

The two-dimensionality of the plume was checked by computing momentum and buoyancy fluxes along the wall, similar to Launder and Rodi (1981). Mean momentum was conserved within ten percent and buoyancy flux was conserved within five percent (Lai, Jeng and Faeth, 1986), although due to turbulent fluxes in variable density, the uncertainty of this conservation check is found to be about six percent for momentum flux and four percent for buoyancy flux (Lai and Faeth, 1987). Aspect ratios, based on displacement, momentum, scalar mixing, and analogous flow widths, were all greater than 10, also suggesting conditions conducive to two-dimensional flow.

Initial profiles of streamwise and fluctuating velocities were measured, and they were similar for all the flows. Ambient stratification could not be reduced below 0.26 $°K/m$ without unduly disturbing the desired stagnant ambient environment of the wall.

THEORETICAL METHODS

The analysis treats a steady two-dimensional vertical wall plume in a stagnant environment having constant properties. Boundary layer approximations are applied, and dissipation and kinetic energy are ignored in the governing equations for mean quantities, with little error. Carbon dioxide and buoyancy are conserved. Typical of most analyses of turbulent mixing, the exchange coefficients are only a function of mixture fraction F (the fraction of mass which originated from the slot). Therefore, passive scalar properties are only a function of the mixture fraction, which is a conserved scalar of the flow.

Turbulent properties were treated using two second-order closure models. Here we consider the model representative of current development. The second-moment closure model is primarily based on the works by Lumley (1978); the scalar transport, Shih, Lumley and Chen (1990); the near-wall treatment, Shih and Mansour (1990, 1992); the pressure-correlation terms; Shih, Shabbir and Lumley (1991). The low-Re SOC model is validated using direct numerical simulation of the fully-developed channel flow. No change of model coefficients is attempted to fit the predictions to the data. In the following section, only the results of model derivations are summarized; details of the derivations can be found in the cited references.

Based on the above assumptions, a system of eleven transport equations (in addition to the conservation equations of mass) are to be solved. These include two conservation equations of mean properties (velocity and mixture fraction F, five modeled equations associated with turbulent momentum transport (Reynolds stress terms $<u^2>$, $<v^2>$, $<w^2>$, $<uv>$ and $<\epsilon>$, which is the dissipation rate of turbulence kinetic energy $<k>$), and four modeled equations associated with turbulent scalar transport (variance of mixture fraction $<f^2>$, its dissipation rate $<\epsilon^f>$, and scalar fluxes $<fu>$ and $<fv>$).

Formulation

Invoking the boundary-layer assumption, the mean continuity, momentum, and mixture fraction equations for the current wall plume calculations are:

$$\frac{\partial \bar{\rho} U}{\partial x} + \frac{\partial \bar{\rho} V}{\partial y} = 0 \tag{1}$$

$$\frac{\partial \bar{\rho} UU}{\partial x} + \frac{\partial \bar{\rho} UV}{\partial y} = \frac{\partial}{\partial y}\left(\mu\frac{\partial U}{\partial y} - \bar{\rho}<uv>\right) - (\bar{\rho} - \rho_\infty)g \tag{2}$$

$$\frac{\partial \bar{\rho} UF}{\partial x} + \frac{\partial \bar{\rho} VF}{\partial y} = \frac{\partial}{\partial y}\left(\alpha\frac{\partial F}{\partial y} - \bar{\rho}<fv>\right) \tag{3}$$

and the density is defined by the state relationship:

$$\frac{1}{\bar{\rho}} = \frac{1}{\rho_0}F + \frac{1}{\rho_\infty}(1 - F) \tag{4}$$

where g is the acceleration of gravity, ρ_0 is the density of the fluid at the slot, and ρ_∞ is the ambient density. Upper case and $< >$ symbols stand for the ensemble-averaged properties and lower case symbols the fluctuating properties.

For simplicity, tensorial notation is used for the following modeled equations.

$$U_k<u_iu_j>_{,k} = -<u_iu_j>U_{j,k} - <u_ju_k>U_{i,k} - [<u_iu_ju_k>$$
$$- c(<q^2u_i>\delta_{jk} + <q^2u_j>\delta_{ik})]_{,k} + 2U_{p,q}(I_{pjqi} + I_{piqj}) + \Pi_{ij}^{(2)}$$
$$- \epsilon_{ij} + <\rho u_j>g_i/\bar{\rho} + <\rho u_i>g_j/\bar{\rho} - (B_{kji} + B_{kij})g_k/\bar{\rho} \tag{5}$$

$$U_k<fu_j>_{,k} = -<fu_j>U_{i,j} - <u_iu_j>F_{,j}$$
$$- (<fu_iu_j> - c'<q^2f>\delta_{ij})_{,j} + 2U_{j,k}I_{ijk}$$
$$- \Pi_i<\epsilon>/<q^2> + <\rho f>g_i/\bar{\rho} - B_{ki}^f g_k/\bar{\rho} \tag{6}$$

$$U_k<f^2>_{,k} = -2<fu_j>F_{,j} - <f^2u_j>_{,j} - 2<\epsilon^f> \tag{7}$$

$$U_k<\epsilon>_{,k} = -<\epsilon u_j>_{,j} - \psi<\epsilon><\tilde{\epsilon}>/<q^2> \tag{8}$$

$$U_k<\epsilon^f>_{,k} = -<\epsilon^f u_j>_{,j} - \psi^f<\epsilon^f>^2/<f^2> \tag{9}$$

where

$$<q^2> = <u_iu_i> \tag{10}$$

$<\epsilon>$ and $<\epsilon^f>$ are the dissipation rate of $<q^2>$ and $<f^2>$:

$$<\epsilon> = <\epsilon_{ii}>/2 = \nu<u_{i,k}u_{i,k}> \tag{11}$$

$$<\epsilon^f> = \alpha<f_{,k}f_{,k}> \tag{12}$$

and

$$<\tilde{\epsilon}> = <\epsilon> - \frac{\nu}{4<q^2>}\left(\frac{\partial <q^2>}{\partial y}\right)^2 \tag{13}$$

c and c' are the model coefficients ≈ 0.2 for the pressure stirring terms (Lumley, 1978).

Attributing to Rotta's (1951) pioneering work, two kinds of interactions contribute to the pressure straining effect, one involving only fluctuating quantities and the other arising from the presence of the mean rate of strain. These two iterations are termed the Return-to-Isotropy (or Slow) part and the Rapid part. In the above equations, the Rapid terms (I_{ijkl} and I_{ijk}), the Return-to-Isotropy terms (Π_{ij} and Π_i), the third-moment terms ($<u_iu_ju_k>$, $<fu_iu_j>$, $<q^2u_i>$, $<f^2u_i>$ and $<q^2f>$), the transport terms in the dissipation rate equations ψ and ψ^f, and the buoyancy terms due

to pressure-correlation (B_{ijk} and B_{ij}^f) need to be modeled. The rapid term in the Reynolds stress equation is modeled by Shih and Lumley (1990) and Shih et al. (1991), as

$$I_{pjqi} = \frac{<q^2>}{30}(4\delta_{pj}\delta_{qi} - \delta_{pq}\delta_{ij} - \delta_{qi}\delta_{pj}) - \frac{<q^2>}{3}(\delta_{qi}b_{pj} - \delta_{pj}b_{qi})$$

$$- \frac{<q^2>}{10}C_{a1}\left(\delta_{pq}b_{ij} + \delta_{ij}b_{pq} + \delta_{qj}b_{pi} + \delta_{pi}b_{qj} - \frac{11}{3}\delta_{qi}b_{pj} - \frac{4}{3}\delta_{pj}b_{qi}\right)$$

$$+ \frac{<q^2>}{10}C_{a2}\left(2\delta_{pj}b_{qi}^2 - 3b_{pq}b_{ij} - 3b_{qj}b_{pi} + b_{qi}b_{pj}\right) \quad (14)$$

where

$$b_{ij} = <u_iu_j>/<q^2> - \delta_{ij}/3 \quad (15)$$

$$C_{a1} = 1 + 0.8\{1 - \exp[(-R_t/40)^2]\}F_I^{1/2} \quad (16)$$

$$C_{a2} = 1 - F_I^{1/2} \quad (17)$$

$$R_t = \frac{<q^2>^2}{9\nu<\epsilon>} \quad (18)$$

and

$$F_I = 1 + 27III + 9II \quad (19)$$

$$II = -\frac{1}{2}b_{ij}b_{ji} \quad (20)$$

$$III = \frac{1}{3}b_{ij}b_{jk}b_{ki} \quad (21)$$

The expression of R_t in C_{a1} is to account for the wall effect and the low-Re nature of the flow (Shih and Mansour, 1990, 1992).

The scalar counterpart of the rapid term is modeled as

$$I_{ijk} = \frac{2}{5}\delta_{ij}<fu_k> - \frac{1}{10}(\delta_{ik}<fu_j> + \delta_{jk}<fu_i>) + C_{D1}b_{ij}<fu_k>$$

$$+ C_{D2}(b_{ik}<fu_j> + b_{jk}<fu_i>) + C_{D3}\delta_{ik}b_{kp}<fu_p> \quad (22)$$

where

$$C_{D1} = \frac{1}{10} + c_1F_D^{1/2} \quad (23)$$

$$C_{D2} = -\frac{3}{10} + c_2F_D^{1/2} \quad (24)$$

$$C_{D3} = \frac{1}{5} + c_3F_D^{1/2} \quad (25)$$

and

$$F_D = \frac{9}{2} - \frac{27}{2}d_{ij}d_{ij} + 9d_{ij}d_{jk}d_{ki} \quad (26)$$

$$d_{ij} = \frac{<f^2><u_iu_j> - <fu_i><fu_j>}{<f^2><q^2> - <fu_p><fu_p>} \quad (27)$$

Model constants c_1, c_2 and c_1 are taken to be 1.8, -1.8 and 4.5 respectively (Shih et al., 1991).

The return-to-isotropy term is modeled together with dissipation rate (Shih and Mansour, 1992), as

$$\Pi_{ij}^{(2)} - \epsilon_{ij} = -\left(\beta b_{ij} + \frac{2}{3}\delta_{ij}\right)<\epsilon>(1 - f_w) - f_w\frac{<\epsilon>}{<q^2>}[2<u_iu_j>$$

$$+ 4(<u_iu_k>n_jn_k + <u_ju_k>n_in_k) + 2<u_ku_l>n_kn_ln_in_j] \quad (28)$$

where

$$\beta = 2 + \frac{F_I}{9}\exp\left(-\frac{7.77}{R_t^{1/2}}\right)\left\{\frac{72}{R_t^{1/2}} + 80.1\ln[1 + 62.4(-II + 2.3III)]\right\} \quad (29)$$

$$f_w = \exp\left[-\left(\frac{R_t}{1.358R_\tau^{0.44}}\right)^2\right] \quad (30)$$

and

$$R_\tau = U_\tau\delta/\nu \quad (31)$$

where U_τ is the shear velocity, δ is the characteristic length scale taken to be distance from the wall to the maximum velocity point y_m.

The scalar counterpart of the slow term is modeled as

$$\Pi_i = \phi^f<fu_i> \quad (32)$$

where

$$\phi^f = \frac{\beta}{2} + r - \frac{(\beta - 2)(1 - d_{ij}d_{ij})/12}{(1 - d_{ij}d_{ij})/6 + d_{ij}b_{jk}d_{ki} - b_{ij}d_{ij}} + HF_D^{1/2} \quad (33)$$

and

$$H = 1.1 + 0.55(\beta - 1)\tanh[4(r - 1)] \quad (34)$$

$$r = \frac{<q^2><\epsilon^f>}{<\epsilon><f^2>} \quad (35)$$

The right-hand-side of the dissipation rate equations is modeled as:

$$<\epsilon u_k> = -\frac{9<q^2>}{5(4\beta + 10)<\epsilon>}<\epsilon>_{,p}\left(<u_ku_p> + \frac{2<u_ku_q><u_pu_q>}{<q^2>}\right) \quad (36)$$

$$<\epsilon^fu_k> = -\frac{<f^2>}{2(1 + \phi^f/r)<\epsilon^f>}<\epsilon^f>_{,p}\left(<u_ku_p> + \frac{<fu_k><fu_p>}{<f^2>}\right) \quad (37)$$

$$\psi = \psi_0 + \psi_1 b_{ij}\frac{<q^2>}{<\epsilon>}U_{i,j} + \psi_2\nu\frac{<q^2>^2}{<\epsilon>^2<\tilde\epsilon>}U_{i,jk}<u_ku_l>(U_{i,jl} - U_{l,j})$$

$$+ \psi_3<\rho u_i>\frac{g_i}{\bar\rho<\epsilon>} \quad (38)$$

$$\psi^f = \psi_0^f + \psi_1^f\frac{<fu_i>}{<\epsilon^f>}F_{,i} \quad (39)$$

where

$$\psi_0 = \frac{14}{5} + 0.98\exp\left(-\frac{2.83}{R_t^{1/2}}\right)[1 - 0.33\ln(1 - 55II)] \quad (40)$$

$$\psi_1 = 2.4 \quad (41)$$

$$\psi_2 = -0.15(1 - F_I) \quad (42)$$

$$\psi_3 = 3.8 \quad (43)$$

$$\psi_0^f = 2 - \frac{2 - \psi_0}{r} - 3\frac{II}{r}\left(\frac{r}{r_e} - 1\right) \quad (44)$$

$$\psi_1^f = \left(2 + \frac{\psi_1 - 2}{r_e}\right)\left(\frac{r_e}{r}\right)^{10} \qquad for \ r < r_e$$

$$\psi_1^f = \left(2 + \frac{\psi_1 - 2}{r_e}\right)\left[1 - 0.1\left(1 - \frac{r_e}{r}\right)\right] \quad for \ r > r_e \quad (45)$$

where the equilibrium time-scale ratio r_e is taken to be 1.6 (Shih, 1990). These modeled terms are found to yield much better results compared with those using the model proposed by Hanjalic and Launder (1976).

The third-moment terms modeled by Lumley (1978) are used in this study.

$$<u_iu_ju_k> = -\frac{<q^2>}{3\beta<\epsilon>}(<u_ku_p><u_iu_j>_{,p}$$

$$+ <u_ju_p><u_iu_k>_{,p} + <u_iu_p><u_ju_k>_{,p})$$

$$+ \frac{\beta - 2}{9\beta}(<q^2u_i>\delta_{jk} + <q^2u_j>\delta_{ik} + <q^2u_k>\delta_{ij}) \quad (46)$$

$$<q^2 u_i> = -\frac{3<q^2>}{(4\beta + 10)<\epsilon>}(<u_i u_p><q^2>_{,p} + 2<u_p u_q><u_i u_q>_{,p})$$

(47)

$$<f u_i u_j> = -\frac{<q^2>}{(\beta + 2\phi^f)<\epsilon>}(<u_j u_k><f u_i>_{,k} + <u_i u_k><f u_j>_{,k}$$

$$+<u_i u_j>_{,k}<f u_k>) + \frac{\beta - 2}{3(\beta + 2\phi^f)}<q^2 f>$$

(48)

$$<q^2 f> = -\frac{<q^2>}{(2 + 2\phi^f)<\epsilon>}(2<u_p u_q><f u_p>_{,q} + <q^2>_{,q}<f u_q>)$$

(49)

$$<f^2 u_k> = -\frac{<f^2>}{(2 + 2\phi^f/r)<\epsilon^f>}(2<f u_p><f u_k>_{,p} + <u_k u_p><f^2>_{,p})$$

(50)

The simpler formulations of Hanjalic and Launder (1976) for $<u_i u_j u_k>$ and $<\epsilon u_k>$ were also tested; the results are very similar.

Finally the buoyancy terms B_{ijk} and B_{ij}^f modeled by Shih et al. (1991) are used in this study without alteration. Their expressions can be found in the reference.

Computation

A parabolic computer program similar to GENMIX (Spalding, 1980) was used to solve the highly-coupled parabolic partial differential equations. However, this program solves modeled transport equations simultaneously rather than sequentially, by using a block-tridiagonal solver. This is to alleviate the problem of numerical instabilities due to the complex coupling of the modeled equations associated with second-order closures. The numerical schemes use a non-staggered grid system to facilitate wall boundary condition treatment. A semi-implicit scheme is applied as the integration is performed downstream. The scheme has a second-order accuracy in the transverse direction and a first-order accuracy in the marching direction.

The boundary conditions are all set identically to zero except for F and $<\epsilon>$ at the wall:

$$U = <u^2> = <v^2> = <w^2> = <uv> = 0$$

$$<f^2> = <fu> = <fv> = <\epsilon^f> = 0$$

$$\frac{\partial F}{\partial y} = 0; \quad <\epsilon> = \frac{\nu}{4<q^2>}\left(\frac{\partial <q^2>}{\partial y}\right)^2 \quad at \ y = 0 \quad (51)$$

For the results presented, fifty grids point was used inside the plume layer. The measured conditions at the exit slot (Lai, 1985) were used as initial conditions in the computation.

RESULTS AND DISCUSSIONS

Since the data for wall plumes are similar, all data used for comparison is for the test case $\rho_o/\rho_\infty = 1.02$. Only the data at the furthest downstream position $z/b = 37.5$ is presented. For convenience, all plotted data and predictions are non-dimensionalized with respect to the maximum mean properties (U_m and F_m) at the particular downstream location, $z/b = 37.5$. To demonstrate the effect of the low-Re treatment, three different implementations were used for comparison. First one is the complete low-Re SOC model as formulated above except for the ψ_1 in Eq. (41) is change from 2.4 to 2.1, as suggested in Shih and Mansour (1990); this is designated as the LL model. Second one, which is designated as the HH model, does not use low-Re treatment at all; i.e., R_t in Eqs. (16) and (29) is set to be infinity and ψ_2 in Eq. (42) is set to be zero for the entire region. Third one, the LH model, implements

low-Re treatment only up to y_m, beyond which the regular high-Re model is used.

Figure 1 shows the comparison between the predictions and measurements for the velocity structure. Interestingly, the HH and LH model predictions are very similar, with the LH slightly better. Both the HH and LH results agree very well with the experimental data, only underpredicting the plume width slightly. This may be why that Lai and Jeng (1990), using simple boundary conditions in earlier SOC model (Lumley, 1978) can predict wall plume with relative success. Both models predict the correct maximum turbulence intensities and Reynolds stress, which is a major success not achieved in previous analysis (Lai et al., 1985-1987). The LL model results do not agree well with the experimental data. It overpredicts the plume width on the free side, while underpredicting the turbulent intensities, suggesting that the turbulence is overdamped. Therefore, Low-Re treatment should not be applied beyond y_m for wall plumes.

Figure 2 shows the comparison between the predicted and measured scalar structure. In general, the agreement is not as well as the velocity structure. The change of sign in the curvatures of F around y_m was more pronouncedly predicted than the original data as reported by Lai (1985). The trends in second- and third-order velocity-scalar correlations, which describe turbulent transport phenomena, are also predicted in general, taking into the account of the larger experimental uncertainty of these measurements. However, the predicted scalar fluctuations are notably lower than the measured levels, with the streamwise correlations worse than the cross-streamwise ones. Underpredicting $<fu>$ will underestimate buoyancy production (Lai and Faeth, 1987) and therefore underestimate the plume width. When comparing the velocity-scalar correlation coefficient results, (i.e., when normalized with respect to the local turbulence quantities $<u_i>$ and $<f>$, rather than U_m and F_m the agreement is much better for all the correlations in the central part of the flow. However, small numerical values of the predicted fluctuations at the outer edge will sometimes cause the correlation coefficients to overshoot beyond unity and violate the Schwarz Inequality. This suggests that the combination of the submodels in the SOC is not completely realizable at the edge; however, this should not cause the large discrepancy observed in the scalar results. The nature of the LDA/LIF measurement may have introduced slightly larger fluctuations in the scalar measurement, since the scattered light from LDA seeding particles may still filter through the long-pass filters and contribute to the fluorescence signal. However, this error has been shown to be small (Lai and Faeth, 1986). A more plausible explanation can be found in the flow visualizations picture and the probability density function (pdf) of the scalar measurements (Lai, 1985). They show large structure of relatively unmixed eddies and deep intermittency spikes penetrating very close to the wall. This may be also why the Low-Reynolds number treatment is not critically important as shown previously.

For comparison, low-Re k-ϵ-f predictions of the wall plumes are also carried out. If low-Re correction is used instead of the wall function for the k-ϵ-f model, one can integrate directly to the wall. The first version of the low-Re k-ϵ model was proposed by Jones and Launder (1972) to predict relaminarization in severely accelerated boundary layer. Since then several authors have proposed alternate versions of low-Re k-ϵ models. Patel et al. (1985) and Bernard (1986) reviewed the performance of the these models for boundary layer flows and found comparative results. All these models have the following basic form:

$$U_j k_{,j} = \left[\left(\nu + \frac{\nu_t}{\sigma_k}\right)k_{,j}\right] + \nu_t U_{i,j}(U_{i,j} + U_{j,i}) - \epsilon - D \quad (52)$$

$$U_j \epsilon_{,j} = \left[\left(\nu + \frac{\nu_t}{\sigma_\epsilon} \right) \epsilon_{,j} \right] + C_{\epsilon 1} f_1 \nu_t U_{i,j} (U_{i,j} + U_{j,i}) \frac{\epsilon}{k}$$
$$- C_{\epsilon 2} f_2 \frac{\epsilon^2}{k} + E \tag{53}$$

where

$$\nu_t = C_\mu f_\mu \frac{k^2}{\epsilon} \tag{54}$$

The model of Chien (1982) is selected for the present study, since it contains only simple algebraic functions and do not involve differential operators and therefore easier to implement. The constants and functions for this model are:

$$C_\mu = 0.09; \quad C_{\epsilon 1} = 1.35; \quad C_{\epsilon 2} = 1.8; \quad \sigma_k = 1.0; \quad \sigma_\epsilon = 1.3 \tag{55}$$

$$f_\mu = 1 - \exp(-0.0115 y^+) \tag{56}$$

$$f_1 = 1.0; \quad f_2 = 1 - 0.22 \exp[-(R_t/6)^2] \tag{57}$$

$$D = 2\nu k/y^2; \quad E = -2\nu(\epsilon/y^2)\exp(-0.5 y^+) \tag{58}$$

For simplicity, buoyancy/turbulence interactions were not considered; only mean momentum equation include the body force term. The computation is performed with fifty grid points in the transverse direction. Turbulent scalar transport term is closed by relating to the turbulent viscosity through a constant turbulent Prandtl/ Schmidt number of 0.9. For comparison, implementation of the wall function is also performed by setting $u^+ = y^+$ since y^+ is very small near the wall. Figure 3 shows the comparison of measurements and predictions by k-ϵ-f models. The result shows that the low-Re model overdamps the plume development beyond y_m, while the results using wall function is better outside, but the development inside y_m is underdamped. The predicted mean mixture fraction is a simple profile as suggested by the gradient-diffusion assumption. The implementation of buoyancy term can not be exact as in the SOC. A switch of the Low-Re treatment in k-ϵ-f near y_m will cause the computation to be unstable. These demonstrate that the limitation of eddy-viscosity isotropic models to predict the flows. However, the performance of turbulence models which are generally validated with high-Reynolds number flows may be limited in their performance in wall plumes.

Figure 4 shows the triple correlation of velocities for the three SOC models. The trend and level of these correlations are similar to those found by Dekeyster and Launder (1983). The profile for the LL model is notably smaller than the other two due to damping of the wall. Without the Low-Re treatment, $<uuv>$ is larger $<vvv>$ for the HH model and part of the LH model results. Figure 5 plots the time-scale ratio profiles. Both LL and HH model show a large variations in the time scale ratio except the LH model, suggesting the deficiency of the LL and HH models in predicting this flow. The equilibrium time-scale ratio r_e is difficult to define theoretically, and the form Eqs. (44) and (45) of is derived crudely. Therefore r_e is considered to be an adjustable constant. Changing the r_e from 1.6 to 4.0 for the LH model shows a more even curve; however, the improvement in the prediction is only slight. The effect of the pressure-correlation buoyancy term in shown in Figure 6. Excluding this extraneously modeled term deteriorate the performance slightly. However, dropping the buoyancy term due to velocity-scalar correlation, which is exact, will degrade the prediction significantly. The measured non-zero boundary conditions for $<u>$, $<v>$ and $<f>$ suggest that a zero-gradient boundary condition for these properties could improve the prediction, as shown in Figure 7.

CONCLUSIONS

A second-order closure simulation of turbulent adiabatic wall plumes, taking into account of the recent progress in scalar transport, near-wall effect and buoyancy, is reported in the current study to compare with the non-intrusive measurements. In spite of the small velocity scale of the wall plumes, the results showed that low-Reynolds-number correction is not critically important for the second-order closure model to predict the adiabatic cases tested and cannot be applied beyond the maximum velocity location. The mean and turbulent velocity profiles are very closely predicted by the second-order closure models. But the scalar field is less satisfactory, with the scalar fluctuation level underpredicted. Strong intermittency of the low-Reynolds-number flow field is suspected of these discrepancies. The trends in second- and third-order velocity-scalar correlations, which describe turbulent transport phenomena, are also predicted in general, with the cross-streamwise correlations better than the streamwise one. Buoyancy terms modeling the pressure-correlation are shown to improve the prediction slightly. The equilibrium time-scale ratio for the wall plumes is found to be around 4. Zero-gradient boundary conditions for the fluctuating velocities and scalar also improve the prediction slightly.

ACKNOWLEDGEMENTS

NOMENCLATURE

B_{ijk}	buoyancy term due to pressure correlation, Eq.(5)
B'_{ij}	scalar buoyancy term due to pressure correlation, Eq.(6)
b	exit slot height
b_{ij}	Eq.(15)
c, c'	model constants, in Eq.(5) and (6)
C_{D1}, C_{D2}, C_{D3}	model coefficients, in Eq.(23)–(25)
$C_\mu, C_{\epsilon 1}, C_{\epsilon 2}$	model constants, in Eq.(61)
c_1, c_2, c_3	model constants, in Eq.(23)-(25)
C_{s1}, C_{s2}	model coefficients, in Eq.(16) and (17)
D	near-wall treatment in k-equation (58), Eq.(63)
d_{ij}	near-wall treatment in Eq.(27)
E	near-wall treatment in ϵ-equation (59), Eq.(63)
F	mean mixture fraction
F_D	function, Eq.(26)
F_I	function of invarients, Eq.(19)
f	fluctuating mixture fraction
f_w	damping function for the slow term, Eq.(30)
f_1, f_2	model coefficients, Eq.(62)
f_μ	damping funtion for Low-Re k-ϵ model, Eq.(62)
g_i	acceleration of gravity
I_{ijkl}	Rapid term, Eq.(14)
I_{ijk}	Scalar Rapid term, Eq.(22)
II	Invarient, Eq.(20)
III	Invarient, Eq.(21)
k	turbulent kinetic energy
q^2	$/\overline{avu_i^2}$ or twice the turbulent kinetic energy, $2k$
Re	Reynolds number
R_t	Reynolds number, Eq.(18)
R_τ	Reynolds number, Eq.(31)

r	time scale ratio, Eq.(35)
r_e	equilibrium time scale ratio, Eqs.(44) and (45)
U, V	mean velocity in (x,y) direction
U_i	mean velocity in the i-direction
U_τ	shear velocity
u_i	fluctuating velocity in the i-direction
u, v, w	fluctuating velocity in the (x,y,z) direction
x	downstream distance from the slot exit
y	normal distance from the wall
y^+	nondimentional normal distance from the wall, $U_\tau y/\nu$
y_m	normal distance from the wall with maximum U
α	diffusion coefficient
β	Eq.(29)
δ_{ij}	Kronecker delta
ϵ	dissipation rate of turbulent kinetic energy, k
ϵ^f	dissipation rate of mixture fraction variance, f^2
ϵ_{ij}	dissipation rate tensor of Reynolds stress, $u_i u_j$
μ	dynamic viscosity
ν	kinematic viscosity
ν_t	turbulent kinematic viscosity, Eq.(60)
$\Pi_{ij}^{(2)}$	slow term, Eq.(28)
Π_i	scalar slow term, Eq.(32)
ρ	density of the fluid
ρ_o	density of the fluid at the slot exit
$\sigma_k, \sigma_\epsilon$	turbulent Prantl/Schmidt numbers, Eq.(61)
ϕ^f	Eq.(35)
ψ	Eq.(38)
$\psi_0, \psi_1, \psi_2, \psi_3$	model coefficients Eq.(40)–(43)
ψ_0^f, ψ_1^f	model coefficients Eq.(44)–(45)
ψ^f	Eq.(39)

Subscript

m	maximum mean properties
0	ambient condition
$( )_{,i}$	$\dfrac{\partial( )}{\partial x_i}$

Superscript

$(\bar{})$	ensemble average
$<>$	ensemble average

REFERENCES

[1] Bernard, P. S. (1986), "Limitations of Near-Wall K-ϵ Turbulence Model," AIAA J., 24(4), pp. 619-622.

[2] Chien, K. Y. (1982), "Predictions of Channel and Boundary-Layer Flows with a Low-Reynolds-Number Turbulence Model," AIAA J., 20, pp. 33-38.

[3] Daly, B. J. and Harlow, F. H. (1970), "Transport Equations of Turbulence," Phys. Fluids, 13, p. 2634.

[4] Dekeyser, I. and Launder, B. E. (1983), "A comparison of Triple-Moment Temperature-Velocity Correlations in the Asymmetric Heated Jet with Alternative Closure Models," Proc. 4th. Symp. on Turbulent Shear Flows, pp. 14.1-14.8, Sept. 12-14, 1983, Karlsruhe.

[5] Gibson, M. M. and Launder, B. E. (1976), "On the Calculation of Horizontal, Turbulent, Free Shear Flows under Gravitaional Influence," J. Heat Transfer, 98, pp. 81-87.

[6] Grella, J. J. and Faeth, G. M. (1975), "Measurement in a Two-Dimensional Thermal Plume along a Vertical Wall," J. Fluid Mech., 71, pp. 701-710.

[7] Hanjalic, K. and Launder, B. E. (1972), "A Reynolds Model of Turbulence and its Application to thin shear layer," J. Fluid Mech., 52, p. 609.

[8] Hanjalic, K. and Launder, B. E. (1976), "Contribution towards a Reynolds-Stress Closure for Low-Reynolds-Number Turbulence," (and Lumley, 1978 and Shih et al, 1987-1991), J. Fluid Mech., 74(4), pp. 593-610.

[9] Hossain, M. S. and Rodi, W. (1977), "Influence of buoyancy on the turbulent intensities in horizontal and vertical jets," in Heat Transfer and Turbulent Convection (ed. D. B. Spalding and N. Afgahan), Hemisphere, New York.

[10] Humphrey, J. A. C. and To, W. M. (1985), "Numerical Prediction of turbulent free convection along a heated vertical flat plate," Proc. 5th Symp. on Turbulent Shear Flows, 22.19-26, Cornell.

[11] Humphrey, J. A. C. and To, W. M. (1986), "Numerical Simulation of Buoyant, Turbulent Flow - II. Free and Mixed Convection in a Heated Cavity," Int. J. Heat Mass Transfer, 29, pp. 593.

[12] Jones, W. P. and Launder, B. E. (1972), "The Prediction of Lamination with a Two-Equation Model for Turbulence," Int J. Heat Mass Transfer, 15, pp. 301-314.

[13] Jeng, S.-M., Chen, L.-D. and Faeth, G. M. (1982), "The Structure of Buoyant Diffusion Methane and Propane Diffusion Flames," 19th Symp. (Int'l) on Comb., The Combustion Institute, Pittsburgh, pp. 349-358.

[14] Jeng, S.-M. and Faeth, G. M. (1984), "Species Concentrations and Turbulent Properties in a Buoyant Diffusion Flames," J. Heat Transfer, 106, pp. 721-727.

[15] Kim, J. and Moin, P. (1987), "Transport of Passive Scalars in a Turbulent Channel Flow," Proc. 6th. Symp. on Turbulent Shear Flows, paper 5.2, Toulouse.

[16] Kruka, V. and Eskinazi, S. (1964), "The wall-jet in a moving stream," J. Fluid Mechanics, 20(4) pp. 555-579.

[17] Lai, M.-C. (1985), "Structure of Turbulent Adiabatic Wall Plumes." Ph.D. Thesis, The Pennsylvania State University, University Park, PA.

[18] Lai, M.-C., Jeng, S. M. and Faeth, G. M. (1986), "Structure of Turbulent Adiabatic Wall Plumes." J. Heat Transfer, 108, pp. 827-834.

[19] Lai, M.-C. and Faeth, G. M. (1987), "Turbulent Structure of Vertical Adiabatic Wall Plumes," J. Heat Transfer, 109, pp. 663-670.

[20] Lai, M.-C. and Faeth, G. M. (1987), "Combined LDA/LIF System for Turbulent Transport Measurements," *J. Heat Transfer*, Vol. 109, pp. 254-256.

[21] Lai, M.-C. and Jeng, S.-M. (1990), "Scalar Transport in Turbulent Wall Plumes and Wall Jets," AIAA paper 90-1735.

[22] Launder, B. E. (1989), "henomenological Modelling: Present ... and Future?" Contributed as a position paper to "Whether Turbulence? or Turbulence at the Crossroads," Cornell University, March 22-24, 1989.

[23] Launder, B. E. and Rodi, E. (1981), "The Turbulent Wall Jet," *Prog. Aerospace Sci.*, 19, pp. 81-128. Launder, B. E. (1983), "The Turbulent Wall Jet - Measurements and Modeling," *Ann. Rev. Fluid Mech.*, 15, pp. 425-459.

[24] Launder, B. E. and Shima, N. (1990), "A Second-Moment-Closure Study for the near-wall sublayer: development and application." To appear in *AIAA J.*

[25] Liburdy, J. A. and Faeth, G. M. (1978), "Heat Transfer and Mean Structure of a Turbulent Thermal Plume along a Vertical Isothermal Wall," *J. Heat Transfer*, 100, pp. 177-183.

[26] Liburdy, J. A., Groff, E. G. and Faeth, G. M. (1979), "Structure of a Turbulent Thermal Plume Rising along a Vertical Isothermal Wall," *J. Heat Transfer*, 101, pp. 249-255.

[27] Lumley, J. L. (1978), "Computational Modeling of Turbulent Flows," *Adv. in Appl. Mech.*, 18, pp. 123.

[28] Lumley, J. L. and Khajeh-Nouri, B. J. (1974), "Computational Modeling of Turbulent Transport," *Advances in Geophysics*, 18A, pp. 169.

[29] Lumley, J. L., Zeman, O. and Siess, J. (1978), "The Influence of Buoyancy on Turbulent Transport," *J. Fluid Mech.*, 84, pp. 581.

[30] McGuirk, J. and Papadimitriou, C. (1985), "Buoyant surface layer under fully entraining and hydraulic jump conditions," Proc. 5th Symp. on Turbulent Shear Flows, 22.33-41, Cornell.

[31] Patel, V. C., Rodi, W. and Scheuerer G. (1985), "Turbulence Models for Near-Wall and Low Reynolds Number Flows,: A Review," *AIAA J.*, 23(9), pp. 1308-1319.

[32] Rogers, M. M., Mansour, N. N. and Reynolds, W. C. (1989), "An algebraic Model for Turbulent Flux of a Passive Scalar," *J. Fluid Mech.*, 203, pp. 77-101.

[33] Rotta, J. Z. (1951), "Staatistche Theorie nichthomogener Turbulenz," *Z. Phys.*, 129, pp. 547-573.

[34] Shima, N. (1988), "A Reynolds-Stress Model for Near-Wall and Low-Reynolds-Number Regions," *J. Fluid Engineering*, 110, pp. 38-43

[35] Shih, T.-S. and Lumley, J. L. (1986), "Second Order Modeling of The Planetary Boundary Layers," CIMMS Report No. 68.

[36] Shih, T.-S. and Lumley, J. L. (1986), "Influence of timescale ratio on scalar flux relaxation: Modeling Sirit & Warhaft's homogeneous passive scalar fluctuations," *J. Fluid Mech.*, 162, pp. 211-222.

[37] Shih, T.-H., Lumley, J. L. and Janicka, J. (1987), "Second-Order Modeling of a Variable-Density Mixing Layer," *J. Fluid Mech.*, 180, pp. 93-116.

[38] Shih, T.-H., Lumley, J. L. and Chen, J.-Y. (1990), "Second-Order Modeling of a Passive Scalar in a Turbulent Shear Flow," *AIAA J.*, 28(4), pp. 609-617.

[39] Shih, T.-H. and Mansour, N. N. (1990), "Modeling of Near-Wall Turbulence," Proc. of Int'l Symp. for Engineering Turbulence Modeling and Measurement, (W. Rodi ed.), pp.13-23.

[40] Shih, T.-H., Shabbir, A. and Lumley, J. L. (1991), "Advances in Modeling the Pressure Correlation Terms in the Second Moment Equations," NASATM104413.

[41] Shih, T.-H. and Mansour, N. N. (1992), "Second-Order Modeling of Low Reynolds Number Turbulence Near-Wall," To appear in *Phys. Fluid*

[42] Spalding, D. B. (1980), "GENMIX: A General Computer Program for Two-Dimensional Parabolic Phenomena", Pergamon Press, Oxford, 1978.

[43] To, W. M. and Humphrey, J. A. C. (1986), "Numerical Simulation of Buoyant, Turbulent Flow - I. Free Convection along a Heated Flat Plate," *Int. J. Heat Mass Transfer*, 29, pp. 573-592.
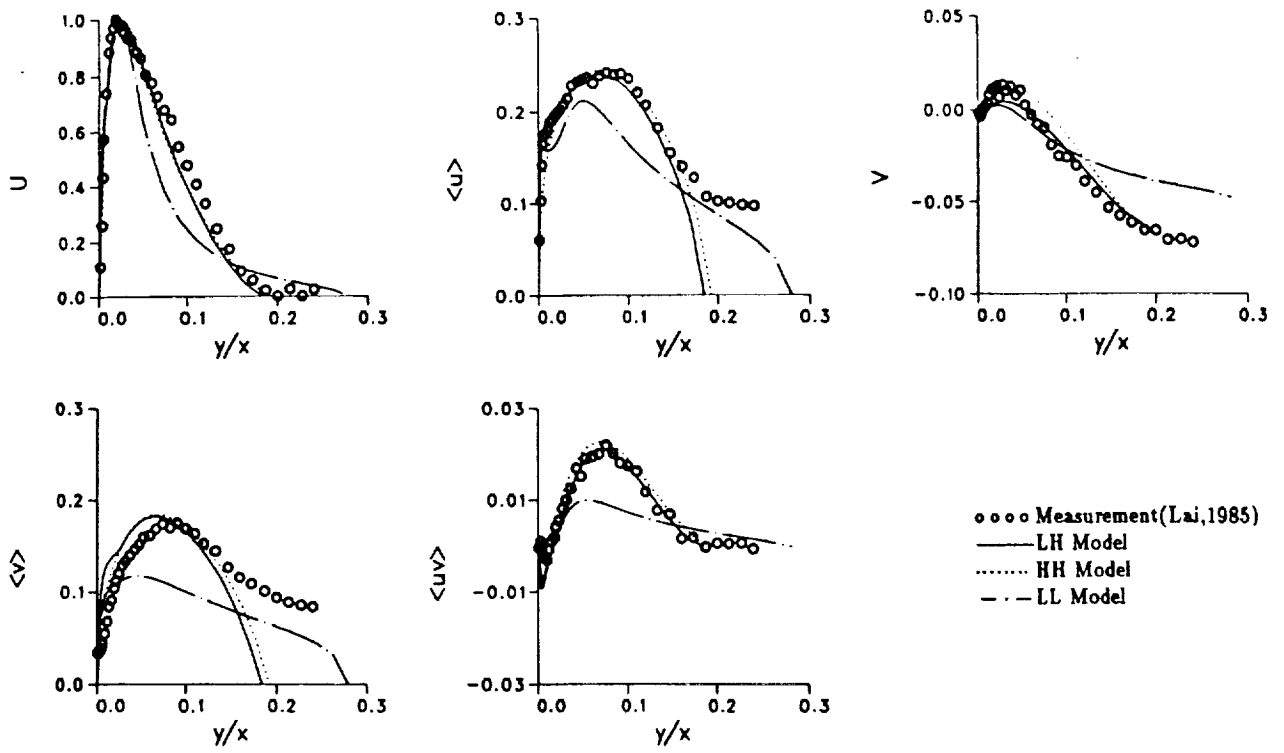
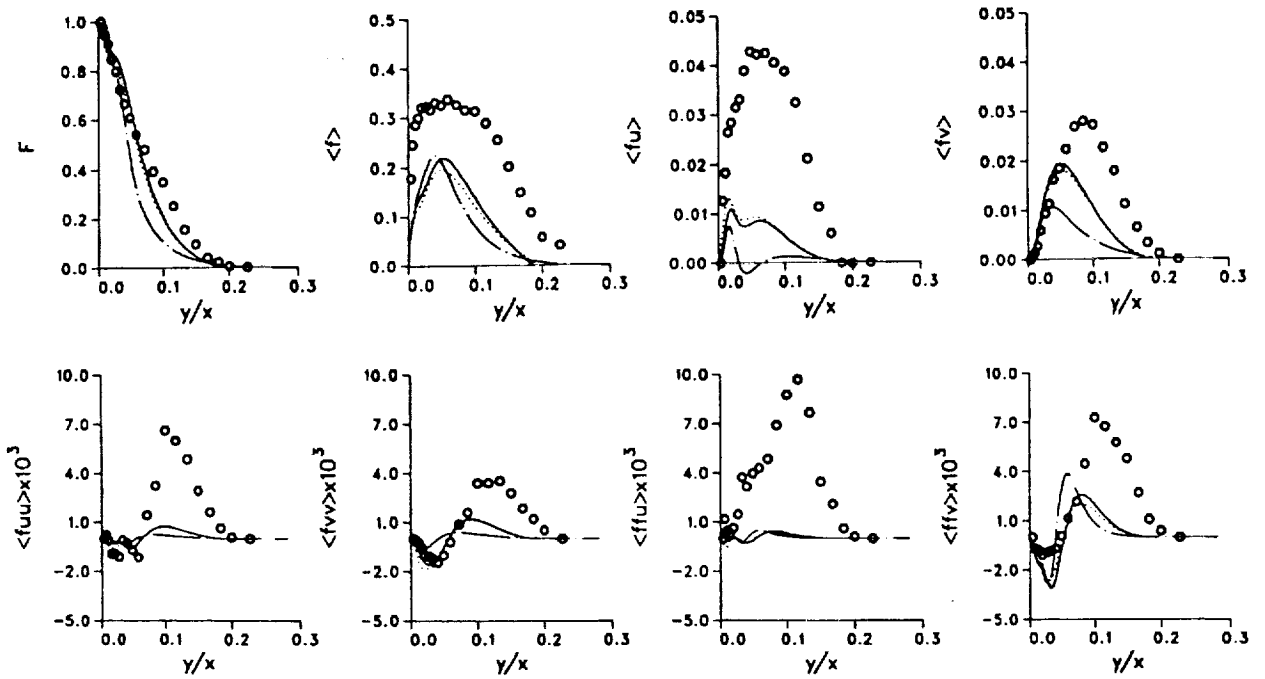Fig.1 Effect of Low-Re Correction on Second-order Closure Model Predictions of Velocity Structure

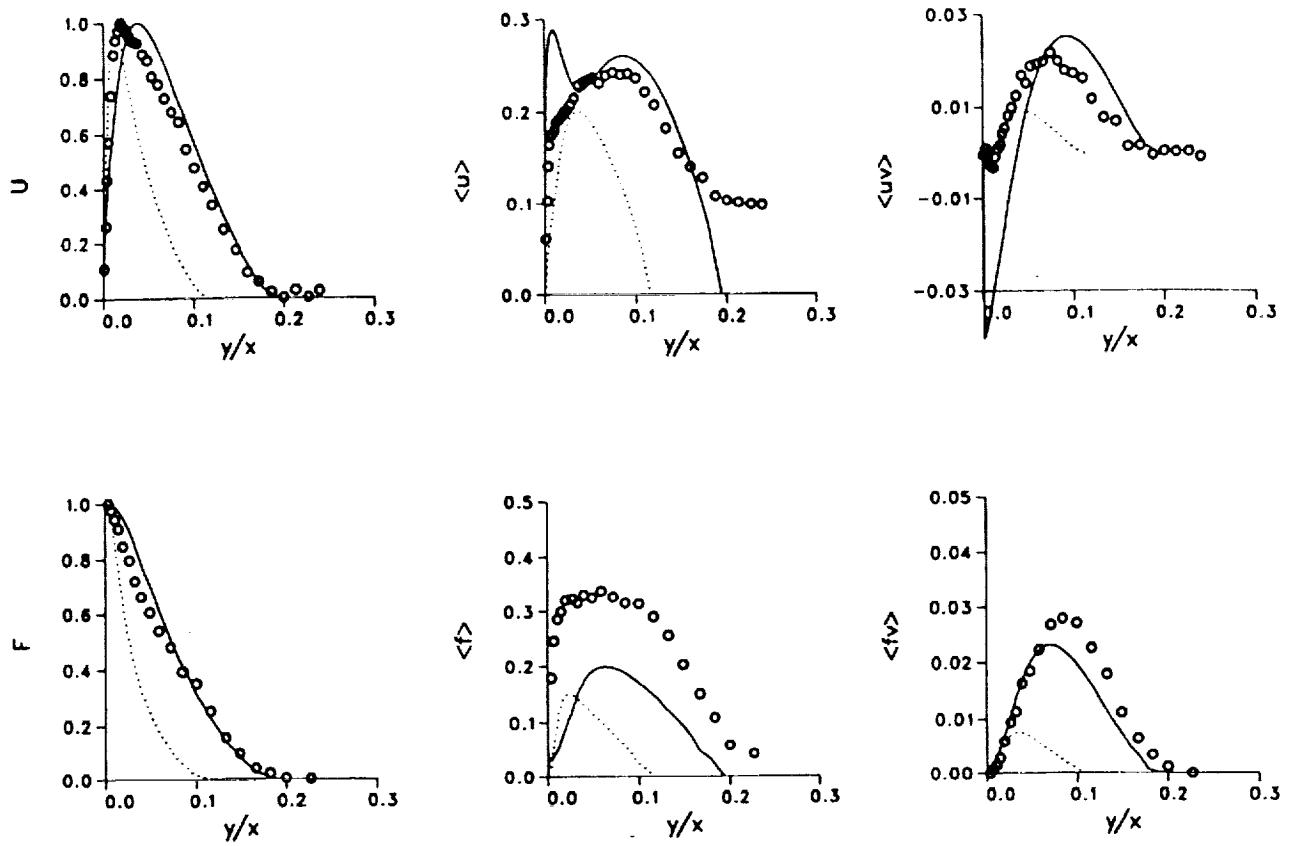Fig.2 Effect of Low-Re correction on Second-order Closure Model Predictions of Scalar

Fig.3 Effect of Low-Re Correction on k-ϵ Model Prediction

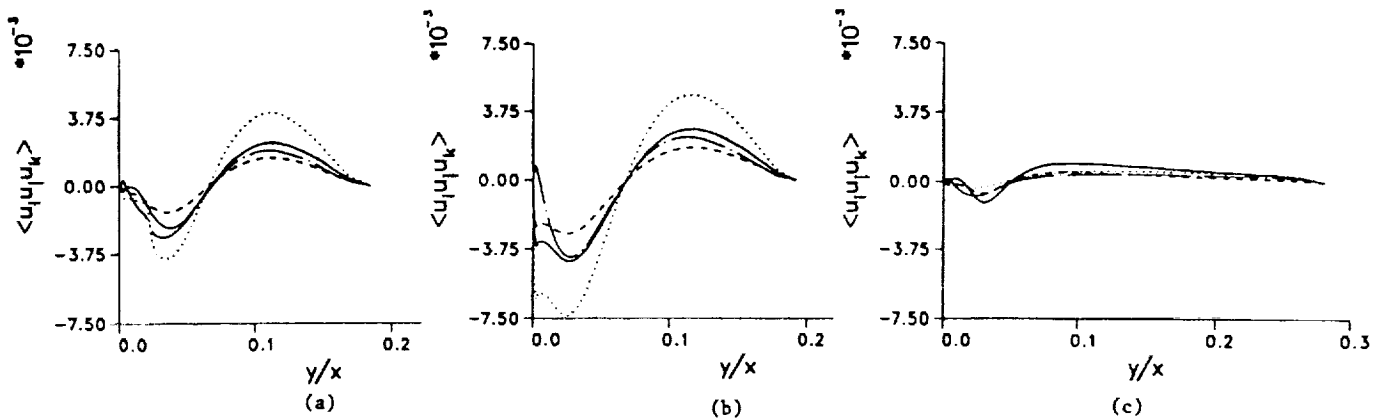———— k-ϵ-f With Wall Function; ········ Low-Re k-ϵ-f

Fig.4 Velocity Tripple Correlation For (a)LH Model; (b)HH Model; (c)LL Model

———— $\langle u_1 u_1 u_2 \rangle$; ········ $\langle u_2 u_2 u_2 \rangle$; – – – $\langle u_3 u_3 u_2 \rangle$; – · – $\langle u_1 u_2 u_2 \rangle$
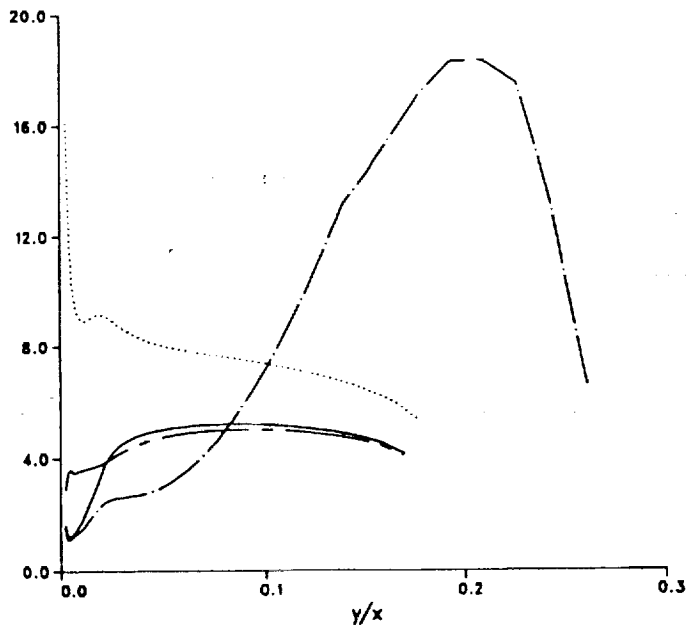
Fig.5 Time Scale Ratio Profile

——— LH Model($r_e = 1.6$) ;   ·········· HH Model($r_e = 1.6$)
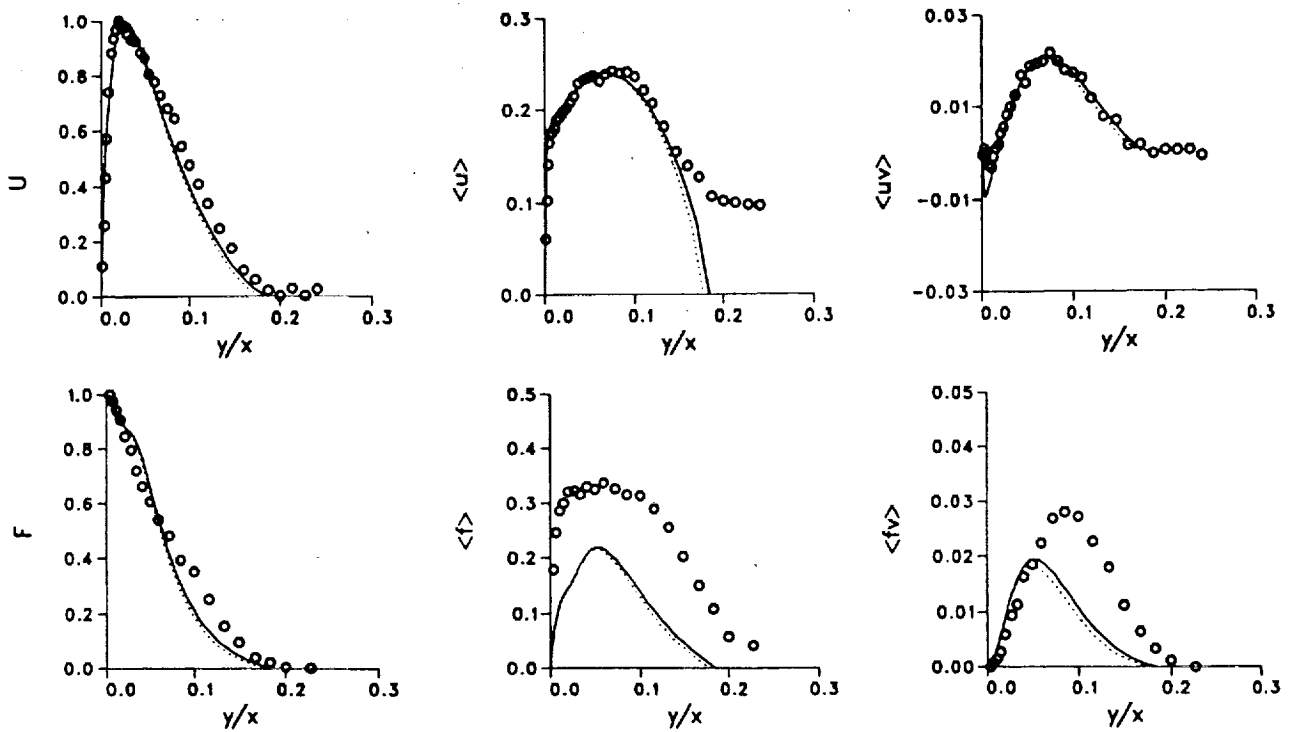— · — LL Model($r_e = 1.6$) ;   — — —LH Model($r_e = 4.0$)

Fig.6 Effect of Pressure-correlation Buoyancy terms

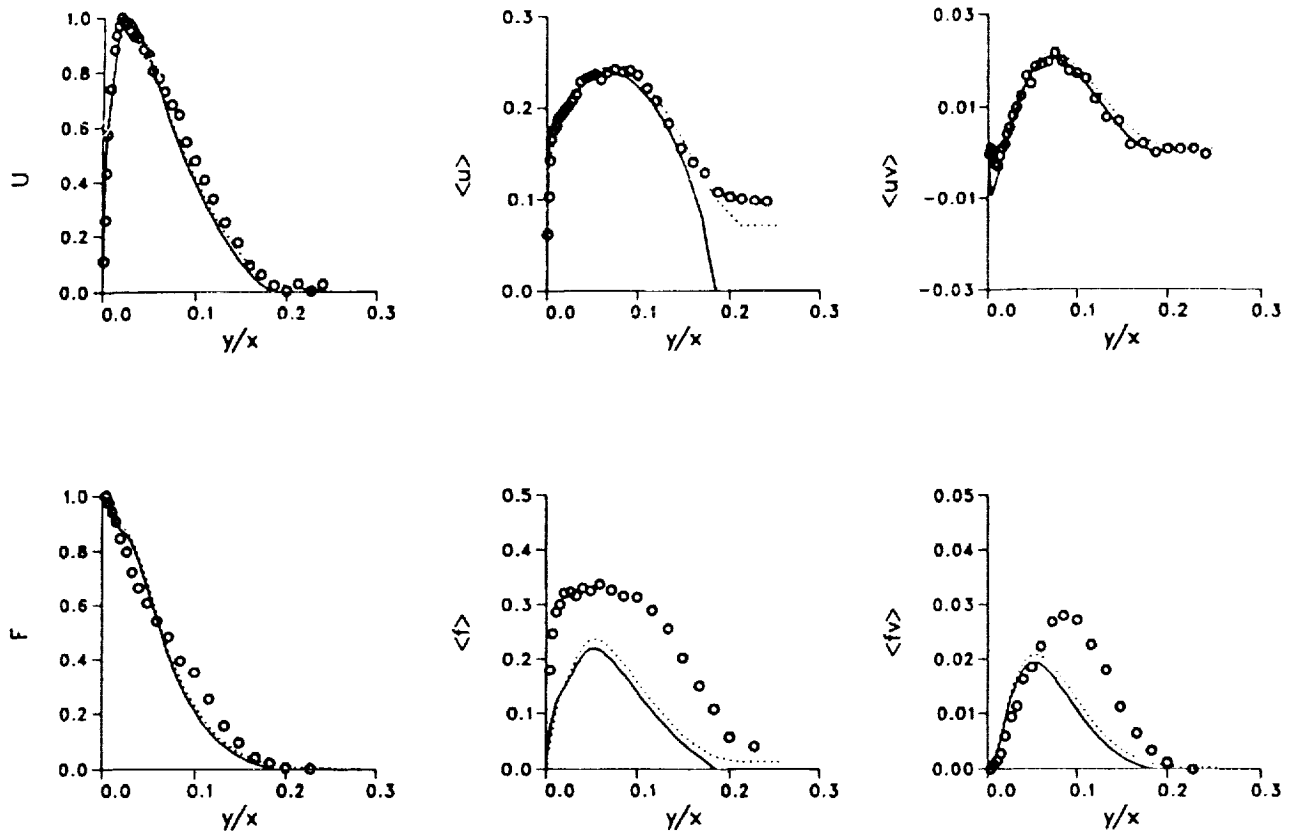——— LH Model With Buoyancy;   ········· LH Model Without Buoyancy

11

Fig.7 Effect of Boundary Condictions

——— Zero B.C. ;   ········ Zero Grad. B.C.

REPORT DOCUMENTATION PAGE

Public reporting burden for this collection of information is estimated to average 1 hour per response, including the time for reviewing instructions, searching existing data sources, gathering and maintaining the data needed, and completing and reviewing the collection of information. Send comments regarding this burden estimate or any other aspect of this collection of information, including suggestions for reducing this burden, to Washington Headquarters Services, Directorate for information Operations and Reports, 1215 Jefferson Davis Highway, Suite 1204, Arlington, VA 22202-4302, and to the Office of Management and Budget, Paperwork Reduction Project (0704-0188), Washington, DC 20503.

1. AGENCY USE ONLY (Leave blank)	2. REPORT DATE	3. REPORT TYPE AND DATES COVERED
	December 1992	Technical Memorandum

4. TITLE AND SUBTITLE

Second-Order Closure Modeling of Turbulent Buoyant Wall Plumes

5. FUNDING NUMBERS

WU–505–62–21

6. AUTHOR(S)

Gang Zhu, Ming-Chia Lai, and Tsan-Hsing Shih

7. PERFORMING ORGANIZATION NAME(S) AND ADDRESS(ES)

National Aeronautics and Space Administration
Lewis Research Center
Cleveland, Ohio 44135–3191

8. PERFORMING ORGANIZATION REPORT NUMBER

E–7476

9. SPONSORING/MONITORING AGENCY NAMES(S) AND ADDRESS(ES)

National Aeronautics and Space Administration
Washington, D.C. 20546–0001

10. SPONSORING/MONITORING AGENCY REPORT NUMBER

NASA TM–105956

11. SUPPLEMENTARY NOTES

Gang Zhu and Ming-Chia Lai, Wayne State University, Detroit, Michigan; and Tsan-Shin Shih, NASA Lewis Research Center, Cleveland, Ohio.

12a. DISTRIBUTION/AVAILABILITY STATEMENT

Unclassified - Unlimited
Subject Category 34

12b. DISTRIBUTION CODE

13. ABSTRACT (Maximum 200 words)

Non-intrusive measurements of scalar and momentum transport in turbulent wall plumes, using a combined technique of laser Doppler anemometry and laser-induced fluorescence, has shown some interesting features not present in the free jets or plumes. First, buoyancy-generation of turbulence is shown to be important throughout the flow field. Combined with low-Reynolds-number turbulence and near-wall effect, this may raise the anisotropic turbulence structure beyond the prediction of eddy-viscosity models. Second, the transverse scalar fluxes do not correspond only to the mean scalar gradients, as would be expected from gradient-diffusion modeling. Third, higher-order velocity-scalar correlations which describe turbulent transport phenomena could not be predicted using simple turbulence models. A second-order closure simulation of turbulent adiabatic wall plumes, taking into account of the recent progress in scalar transport, near-wall effect and buoyancy, is reported in the current study to compare with the non-intrusive measurements. In spite of the small velocity scale of the wall plumes, the results showed that low-Reynolds-number correction is not critically important to predict the adiabatic cases tested and cannot be applied beyond the maximum velocity location. The mean and turbulent velocity profiles are very closely predicted by the second-order closure models. But the scalar field is less satisfactory, with the scalar fluctuation level underpredicted. Strong intermittency of the low-Reynolds-number flow field is suspected of these discrepancies. The trends in second- and third-order velocity-scalar correlations, which describe turbulent transport phenomena, are also predicted in general, with the cross-streamwise correlations better than the streamwise one. Buoyancy terms modeling the pressure-correlation are shown to improve the prediction slightly. The effects of equilibrium time-scale ratio and boundary condition are also discussed.

14. SUBJECT TERMS			15. NUMBER OF PAGES
Turbulence modeling; Wall plumes			14
			16. PRICE CODE A03

17. SECURITY CLASSIFICATION OF REPORT	18. SECURITY CLASSIFICATION OF THIS PAGE	19. SECURITY CLASSIFICATION OF ABSTRACT	20. LIMITATION OF ABSTRACT
Unclassified	Unclassified	Unclassified	